UNIAXIAL COMPRESSION SIMULATION USING DISCRETE ELEMENTS AND PARALLEL PROCESSING

Luiz Carlos Facundo Sanches

lsanches@sjbv.unesp.br

São Paulo State University - UNESP

Av. Profª. Izette Corrêa Fontão, 505, 13.876-750, São Paulo, São João da Boa Vista, Brazil

Ronaldo Carrion

rcarrion@usp.br

University of São Paulo - USP

Av. Prof. Luciano Gualberto, travessa 3, 380, 05508-010, São Paulo, São Paulo, Brazil

Carlos Héracles Moraes de Lima

carlos.lima@sjbv.unesp.br

São Paulo State University - UNESP

Av. Profª. Izette Corrêa Fontão, 505, 13.876-750, São Paulo, São João da Boa Vista, Brazil

Abstract. *This paper studies macroscopic properties in geomaterials samples using Discrete Element Method (DEM) and parallel computing. In an uniaxial compression experiment, a sample of geomaterial is slowly compressed by a piston until failure occurs. The peak stress at which failure of the sample occurs is known as Unconfined Compressive Strength (UCS). Analytical relationship between the microphysical parameters and the macroscopic properties are obtained by conducting a series of simulations to tune the microphysical parameters until desired macroscopic properties. For each particle, the interaction law is used in conjunction with the momentum balance principle so as to specify a set of governing equations to describe its interactions and motion. By solving this equations, we obtain the final state of rest of these particles. In our numeric simulation, a rectangular prism of particles is placed between two piston walls which are compressed at constant speed. Then, we monitor the positions, forces and the number of broken bonds. These data is used to measure the macroscopic elastic properties of the particle model. Results show that algorithms have high scalability in CPU-based multi-thread parallel computing and it is possible to obtain some macroscopic properties of geomaterials.*

Keywords: *Computational Geomechanics, Uniaxial Compression Simulation, Geomaterials, Discrete Elements, Parallel Processing*

Proceedings of the XXXVIII Iberian Latin-American Congress on Computational Methods in Engineering P.O. Faria, R.H. Lopez, L.F.F. Miguel, W.J.S. Gomes, M. Noronha (Editores), ABMEC, Florianópolis, SC, Brazil, November 5-8, 2017.

1 INTRODUCTION

In the field of Geotechnics or Geomechanics, well-known geomaterials, like rocks, concretes or soils, exhibit similar constitutive response when considering their yield strength dependencies or dilatancy processes. Their discontinuous and inhomogeneous nature leads to complex mechanical behaviors which can be difficult to capture with standard numerical models as finite or boundary elements (Donzé et al., 2009).

Continuous description of geomaterials encounters limitations when large-scale slip and opening of a large amount of fractures. An alternative is to use discrete-based methods which represent the material as an assemblage of independent elements (also called units, particles or grains), interacting with one another. Such models explicitly reproduce the discrete nature of the discontinuities, which are represented as the boundary of each element. Discrete Element Method (DEM) are numerical methods for discrete systems made of non-deformable elements and particularly suitable to model granular materials. This method was initially described by Cundall and Strack (1979) and has been widely used in dynamic numerical analyses from an engineering perspective. The scheme is a *Lagrangian* approach where individual particles are calculated on the basis of *Newton's* second law of motion. Discrete or distinct elements enable us to investigate the dynamic characteristics of particles and their motion precisely. For example, DEM application in a discontinuous medium was accomplished by Hoang Tran (2013) that demonstrated the method efficiency in modeling the behavior of granular soil domains in microscopic scale.

In the aforementioned problems, numerical computation becomes costly when the number of these particles is very large. Thus novel modeling and parallel calculation techniques are needed to implement better practical DEM in complicated and large scale systems. Lately, powerful computer clusters and super computers have been used to simulate complex systems with large number of constituent particles using DEM. However, their excessive deployment costs limit their popularity. Similar results have been reported for other applications, *e. g.*, computational fluid dynamics, structural analyses, and rigid body simulations. In these cases, the number of cores available on a central processing unit (CPU) has been steadily increasing as well. Recently multi-core processors for both graphics processing unit (GPU) and latest multi-core CPU, have emerged as a promising low-cost alternative to enable multi-thread parallel computations (Sakai et al., 2010). Munjiza et al. (2012) performed the analysis of a solids mechanics problem with discrete elements and observed that DEM is computationally expensive. However, they said that the reconfigurable computing can be used to make it less demanding.

In this paper, we will investigate how to implement a uniaxial compression simulation using DEM and parallel processing. The simulations measure the equivalent macroscopic properties of synthetic geomaterials samples and can be an important tool for calibrating discrete element models. In fact, a quasi-static uniaxial compression test of a geomaterial sample is a common laboratory technique for measuring the macroscopic properties such as *Young's* modulus, *Poisson's* ratio and the Unconfined Compressive Strength (UCS). The last property is an important measure of the strength of a geomaterial and is associated to the peak stress at which failure of the sample occurs (Weatherley et at., 2014).

Proceedings of the XXXVIII Iberian Latin-American Congress on Computational Methods in Engineering
P.O. Faria, R.H. Lopez, L.F.F. Miguel, W.J.S. Gomes, M. Noronha (Editores), ABMEC, Florianópolis, SC, Brazil, November 5-8, 2017.

The *Young's* modulus and the UCS were obtained from a stress-strain curve. *Young's* modulus is defined as the slope of the linear section of the stress-strain curve, whilst the UCS is the corresponding peak value. Equally important, the number of broken bonds is a useful quantity to monitor in elastic-brittle simulations, as measures of amount of damage the geomaterial sample has suffered due to the external load. Time-series of the number of broken bonds are presented along with the wall force time-series for comparison.

Usually, is difficult to establish an analytical relationship between the microphysical parameters and the macroscopic properties of the material. To overcome this, it is a common procedure to conduct uniaxial compression simulations to fine tune the microphysical parameters until suitable macroscopic properties are obtained.

2 METHODOLOGY

Traditional DEM was developed by Cundall and Strack (1979) which considered an explicit solution for the dynamic equilibrium of individual particles rather than solving the entire system. The equations governing the translational and rotational dynamic equilibrium of a particle *i* with mass m_i is

$$\frac{d^2 x_i(t)}{dt^2} = \ddot{x}_i(t) = \frac{F_{xi}(t)}{m_i}, \tag{1}$$

$$\frac{d^2 \theta(t)}{dt^2} = \ddot{\theta}_i(t) = \dot{\omega}_i(t) = \frac{T_i(t) + M_i(t)}{I_i}, \tag{2}$$

where $\ddot{x}_i$ is the acceleration vector for *ith* particle, F_{xi} are the contact forces, m_i is the particle mass, $\dot{\omega}_i$ is the angular velocity vector, T_i is the torque, M_i is the resultant moment acting through the centroid of the particle *i* and I_i is the moment of inertia. For a circular particle the moment of inertia is equal to $\rho \pi r_i^4 / 2$ where r_i is the radius and ρ is the density.

2.1 Updating particle position

From the dynamic equilibrium equations of particles and knowing the resulting forces acting on them, it is possible to calculate the accelerations for *ith* particle. Particularly, if the translation motion, can be isolated, we have:

$$m_i a_i^t = F_i^t, \tag{3}$$

where m_i is the inertia (mass) matrix, $a_i^t = \ddot{u}_i^t$ is the acceleration vector at time *t*, and F_i^t is the resultant force vector. To update such parameters it is necessary to implement integration methods, i.e. given by their first and second derivatives with respect to time.

With DEM, the relationship between the acceleration and velocity vector is:

$$a_i^t = \frac{1}{\Delta t}\left(v_i^{t+\Delta t/2} - v_i^{t-\Delta t/2}\right), \tag{4}$$

where $v_i^{t-\Delta t/2}$, $v_i^{t+\Delta t/2}$ are the velocity at $t - \Delta t/2$ and $t + \Delta t/2$ respectively for the *ith* particle.

Equation (4) is also known as the position *Verlet* time integration scheme, and the velocity at time $t + \Delta t/2$ is then calculated as:

$$v_i^{t+\Delta t/2} = v_i^{t-\Delta t/2} + \Delta t \frac{1}{m_i}\left(F_i^t\right). \tag{5}$$

The velocity at time $t + \Delta t/2$ is equal to the average velocity within the interval from t to $t + \Delta t$. Then, we can calculate the updated particle position as:

$$x_i^{t+\Delta t} = x_i^t + \Delta t \times v_i^{t+\Delta t/2}, \tag{6}$$

where the particle position vector x gives the particle Cartesian coordinates and the total rotation about the principal axis (for the 3D case). In two dimensions there is no coupling between the three degrees of rotational freedom.

2.2 Calculating contact forces

The force F_n denotes the normal component of the contact force, while the tangential (shear) component is denoted by F_t. The contact normal force can be calculated as (O'Sullivan, 2011):

$$F_n = F_N - c_n v_n, \tag{7}$$

where F_N is the elastic part of the normal interaction, c_n is the normal interaction damping coefficient, $v_n = (v \cdot n)n$ if n is the unit vector in the interaction between the centers of the two particles, v is the particle translational velocity vector.

The second term on the right-hand side of Eq. (7) represents the contact damping. There is also a tangential interaction, the frictional component of which is given by

$$F_T = \mu F_N \left(1 - \left(1 - |\delta_t| / \delta_{máx}\right)^{3/2}\right), \tag{8}$$

where δ_t is the total tangential displacement between the two surfaces from the point where they initially came into contact. If $|\delta_t| > \delta_{máx}$ then gross sliding is deemed to have started and the frictional force assumes a constant value given by *Amonton's* law, $F_T = \mu F_N$, where μ is the friction coefficient. The total tangential (shear) interaction force at any time is

$$F_t = F_T - c_t v_t. \tag{9}$$

The second term on the right-hand side of Eq. (9) is the contact damping force proportional to the tangential component of the relative velocity, $v_t = v \times n$ and c_t is the tangential interaction damping coefficient.

2.3 Rotational bonds and frictional interactions

To simulate geomaterials failure under compressive loads, we need to integrate some additional techniques to traditional DEM, as listed below:

1. Implementation of cementations (rotational) elastic-brittle bonds and rotational friction interactions,
2. Moving walls,

The model adopted consists of a rectangular prism of particles sandwiched between two piston walls, which are compressed at constant speed. Simulation results are then used to measure the macroscopic elastic properties of the particle model. A typical particle interactions model is designed for only three (translational) degrees of freedom configuration and is suitable for granular flow of individual particles or aggregates. To simulate elastic-brittle failure of geomaterials, more sophisticated particle-pair interactions are required. In particular, a particle-pair interaction that incorporates both translational and rotational degrees of freedom is required. As illustrated in Figure 1, two bonded particles may undergo normal and shear forces, as well as bending and twisting moments. According to Weatherley et al. (2014), bonds designed to impart such forces and moments are known as cementations bonds.

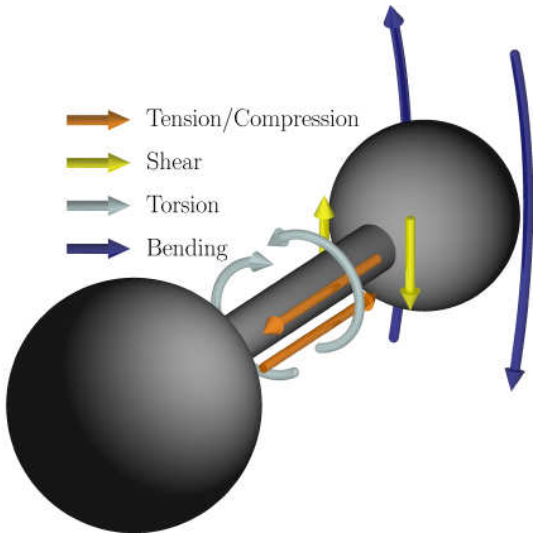

Figure 1. Forces and moments between particles bonded via rotational elastic-brittle bonds (Weatherley et al., 2014).

In order to properly simulate elastic-brittle failure, bonds require a failure threshold criterion. In this work a *Mohr-Coulomb* failure criterion is employed. A bond will fail if the shear stress within the bond exceeds its shear strength τ, given by:

$$\tau = C + \sigma_N \tan(\varphi_f), \tag{10}$$

where C is the cohesive strength of the bond for zero normal stress σ_N and φ_f is the internal angle of friction of the bond.

2.4 Implementation of viscous damping

Uniaxial compression experiments are usually conducted in the so-called quasi-static regime, *i. e.*, external loads are applied slowly compared with the compressional wave speed of the sample. To simulate these conditions, it is also necessary to incorporate two body forces designed to attenuate translational and rotational oscillations. The viscosity coefficients are chosen to be small so that damping has little effect on the elastic response of the simulated geomaterial sample but it is sufficient to attenuate unwanted oscillations.

2.5 Macroscopic elastic properties

Macroscopic elastic properties as *Young's* modulus and Unconfined Compressive Strength (UCS) can be obtained from a stress-strain curve. To measure these quantities in a simulation, it is necessary construct the stress-strain curve for the geomaterial. Therefore, suppose the net restoring forces (at time *t*) that particles apply to the top and bottom walls are $F^{(t)}(t)$ and $F^{(b)}(t)$ respectively, and the unit normal vector of the walls is $n^{(t/b)}$. The stress exerted on the walls by the particle assembly is:

$$\sigma_{YY}(t) = \frac{F^{(t)} \cdot n^{(t)} + F^{(b)} \cdot n^{(b)}}{2A_c}, \tag{11}$$

where A_c is contact area between a wall and the particle assembly. Since the peak stress is reached for relatively small axial strain, the contact area can be approximated by the undeformed area at particle assembly base.

It is also relatively straightforward to accounting for the total strain. Let $X(t)(t)$ and $X(b)(t)$ be the positions of the top and bottom walls at time *t*. The strain $\varepsilon_{YY}(t)$ is given by:

$$\varepsilon_{YY}(t) = \frac{\left[\left(X^{(t)}(0) - X^{(b)}(0)\right) - \left(X^{(t)}(t) - X^{(b)}(t)\right)\right] \cdot y}{\left[\left(X^{(t)}(0) - X^{(b)}(0)\right)\right] \cdot y}, \tag{12}$$

or

$$\varepsilon_{YY}(t) = 1 - \frac{\left[\left(X^{(t)}(t) - X^{(b)}(t)\right)\right] \cdot y}{\left[\left(X^{(t)}(0) - X^{(b)}(0)\right)\right] \cdot y}, \tag{13}$$

where *y* is the unit vector normal to the bottom wall. To compute the stress-strain curve, we use the net force acting on each wall and their position at each simulation time step.

2.6 Adding walls to the simulation

We add two walls, which serve as pistons for compressing the geomaterial sample. One of them is added below the sample (the bottom wall) and another atop the sample (the top wall). It is worth mentioning that simply adding walls to the simulation is insufficient, we also have to define interactions between the walls and particles. For basic uniaxial compression simulations, repulsive elastic interactions are enough. If the interest were in tensile loading, one would need to bond the walls to particles at the base and top of the model. Herein, the following particle-wall interactions are sufficient to carry out simulations.

2.7 Implementation of moving walls

Only one component remains to be added to the uniaxial compression simulation: a method to move the two walls at constant speed. In this case, the wall speed is linearly increased from zero to the desired value over a few hundred time-steps. The top wall will move downwards and the bottom wall upwards.

3 DEM PARALLEL PC MULTI-CORE PROCESSORS

Traditionally, the vast majority of software applications were written as sequential programs (von Neumann, 1945) and historically, computer users had the expectation that these programs would run quicker as new generation of microprocessors arises. Without improving performance, application developers were not able to introduce new capabilities into their software as new processors are introduced, thereby reducing the growth opportunities of the computer industry. Thus, applications that needed a performance increase would be through parallel programs, in which multiple ways of execution allow a faster work. The High Performance Computing (HPC) community has been developing parallel programs for decades and now that all processors are parallel computers, the number of applications has grown dramatically. Since 2003, the semiconductor industry has been working on two main trends to develop microprocessors (Hwu et al., 2008). The first, called multi-core, seeks to maintain the execution speed of sequential programs, but in the direction of multiple cores that started with two processors with number of cores doubling each generation of semiconductors. The second one, called many-core, deals with the execution of parallel applications that began with a large number of several small cores and also doubles each generation.

This work is based on multi-core processing. A modular open source object-oriented simulation code written in C was tested. The DEM simulation includes registering particles and walls, collision detection, calculating the contact force, and updating particles. According to Weatherley et al. (2010), spatial domain decomposition (in sub-domains) is implemented using a master slave strategy with inter process communications using the Message Passing Interface (MPI). For this, a *Verlet* list neighbor search algorithm for detecting neighboring particles and an explicit first-order finite difference time integration scheme is employed. Besides, a simple Application Programming Interface (API) allows evaluating simulations via scripts written in Python programming language. During all iterations and loading step, each DEM ensemble runs independently. The parallelization is achieved by decomposing the problem domain into sub-domains, where the interface of each sub-domain needs to be duplicated for information to be passed between two neighboring sub-domains.

The computer simulations ran in Linux Ubuntu 14.02 and simulation was made in personal computer using multi-core CPU. Processing was implemented in an Intel Sandy Bridge Core i7 2600 with Seven-Core Processor, 3.40 GHz Quad Box CPU clock and system with 8.0 GB RAM.

4 NUMERICAL RESULTS

At initialization, particles are randomly inserted and bond together. For geomaterials breakage simulations, the best results are obtained using blocks of particles with variable radii and random locations. The simulation scenario generates a rectangular prism of particles whose radii lie in the range 0.4 until 2.0 mm. The prism is 10 x 20 x 10 mm in size with the center of the base at the origin. Each particle pair is tagged with a bond tag that specifies the type of interactions between bonded particles. Next, two walls are added to the simulation scenario. As previously said, these walls serve as pistons for compressing the geomaterial sample which are positioned below (bottom wall) and above the sample (top wall). Then,

interactions between the walls and particles are defined: repulsive elastic interactions are sufficient for basic uniaxial compression simulations under study. However, we would need to bond the walls to particles at the base and top of the model to assess tensile loading. The elastic stiffness (a single microphysical parameter) specifies the elastic repulsion between sample particles and walls. For this simulation we set the elastic stiffness equal to 102,000.0 N/mm^2.

To simulate elastic-brittle failure, more sophisticated particle-pair interactions are required. In particular, particle-pair interactions that incorporate both translational and rotational degrees of freedom. Then, two bonded particles may undergo normal and shear forces, as well as bending and twisting moments. Bonds designed to impart such forces and moments are known as cementations bonds. Rotational frictional interactions are defined by a microscopic *Young's* modulus equal to 100,000.0 N/mm^2 and *Poisson's* ratio equal to 0.25 and two microscopic coefficients of friction. Typically the *Young's* modulus and *Poisson's* ratio for friction interactions are set equal to their brittle counterparts. The static M_u coefficient of friction is set 0.6 and applied when two particles are in static frictional contact, i.e., prior to the first time the frictional sliding criterion is met. Thereafter the dynamic M_u coefficient of friction equals 0.4 is applied. By setting dynamic M_u < static M_u, one can simulate the physical observation that the frictional force required to maintain sliding is less than the force necessary to initiate sliding. A viscosity coefficient equal to 0.002 is chosen small so that damping has little effect on the sample elastic response, but is still sufficient to attenuate unwanted oscillations.

Finally, in the uniaxial compression simulation, we move the two walls at constant speed. It is best to gradually increase the wall speed from zero to the desired value over a few hundred timesteps. The velocity of the wall increases linearly over that number of timesteps. In addition, the two walls move in opposite directions both at a speed of 0.125 m/s. Although this rate is significantly higher than typically used in laboratory uniaxial compression experiments, it is sufficiently small to maintain quasi-static conditions in our simulations. The piston speeds are approximately 20000× lower than the compressional wave speed of the simulated geomaterial sample. The initial acceleration of the walls from zero to the desired speed (during the first 50000 timesteps) also helps ensure the sample is loaded quasi-statically (Weatherley et al., 2014).

4.1 Measurement of macroscopic elastic properties

The *Young's* modulus and Unconfined Compressive Strength (UCS) was obtained from a stress–strain curve, as shown in Figure 2. In this evaluation scenario, *Young's* modulus is equal to 188 GPa and corresponds to the slope of the linear section of the stress–strain curve, whilst the UCS is equal to 299.9 MPa and given by the stress peak value. Considering magnitude the values found, it is possible to relate this sample of geomaterial analyzed with a rock material or a high resistance concrete.

It is also feasible to determine the time series of the broken bonds between particles, as well as the force exerted on the rigid wall. Figure 3 shows that the maximum force on the bottom wall occurs between 15000 and 20000 step increments (loading and unloading).

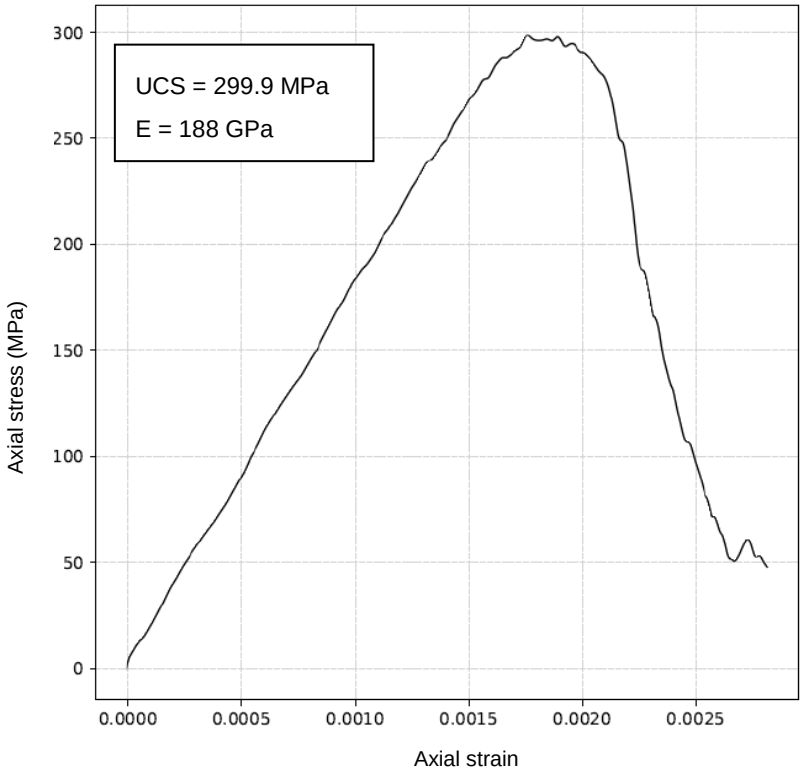

Figure 2. Stress-strain curve obtained from a uniaxial compression simulation.

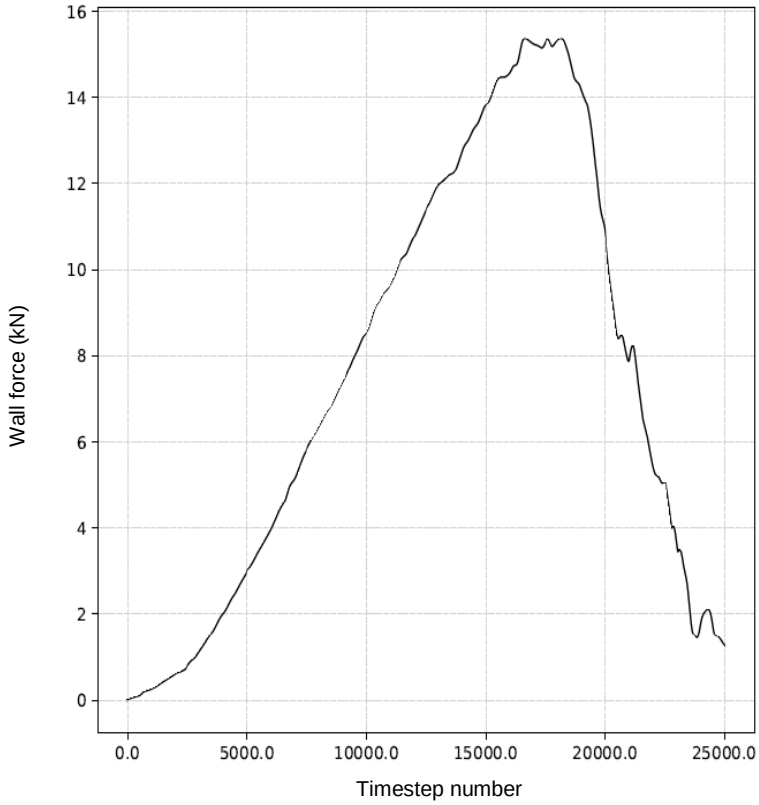

Figure 3. Time-series of net wall force during a uniaxial compression simulation.

From Figure 4, we can evaluate time series of the broken bonds in the connected particles. First, it is evident that a significant fraction of bonds breaks down before the peak stress is reached. In other words, the sample undergoes significant irreversible internal damage before reaching UCS. The second interesting observation is that the total number of broken links after the peak stress is reached is approximately 35% of the initial number of connections.

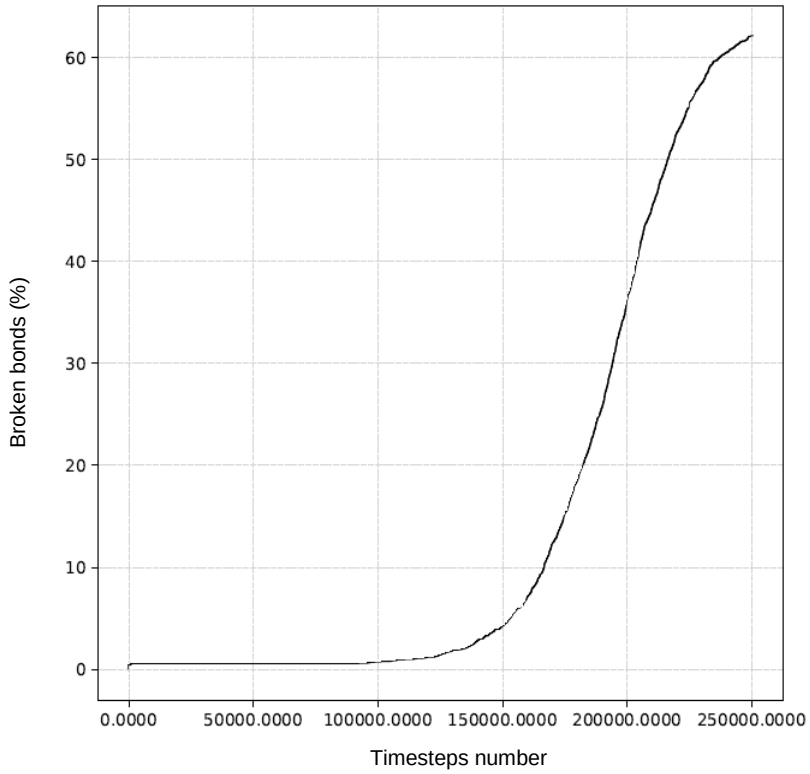

Figure 4. Time-series of percentage of bonds broken during a uniaxial compression simulation.

Considering the results presented previously, we observed that the geomaterial sample remains largely intact even after the post-peak stress. This is exactly what one would expect in laboratory uniaxial compression experiments.

A second analysis was made considering only an increase in the particle size of the material (ranging of 0.8 until 4.0 mm). A variation of the UCS and the *Young's* modulus (E) can be observed in Figure 5. Now, we observe a decrease in resistance as a result of the particle size increase. Similarly, it is possible to determine the time series of the force exerted on the rigid wall for the material with larger particles. Figure 6 shows again that the maximum force on the bottom wall occurs between 15000 and 20000 step increments with a small maximum peak displacement. However, the maximum force value decreases by about 20%. Finally, the time series of the particles broken bonds for this case is shown in Figure 7. We see that the total number of broken bonds after reaching the maximum force undergoes a reasonable variation from the initial number of connections.

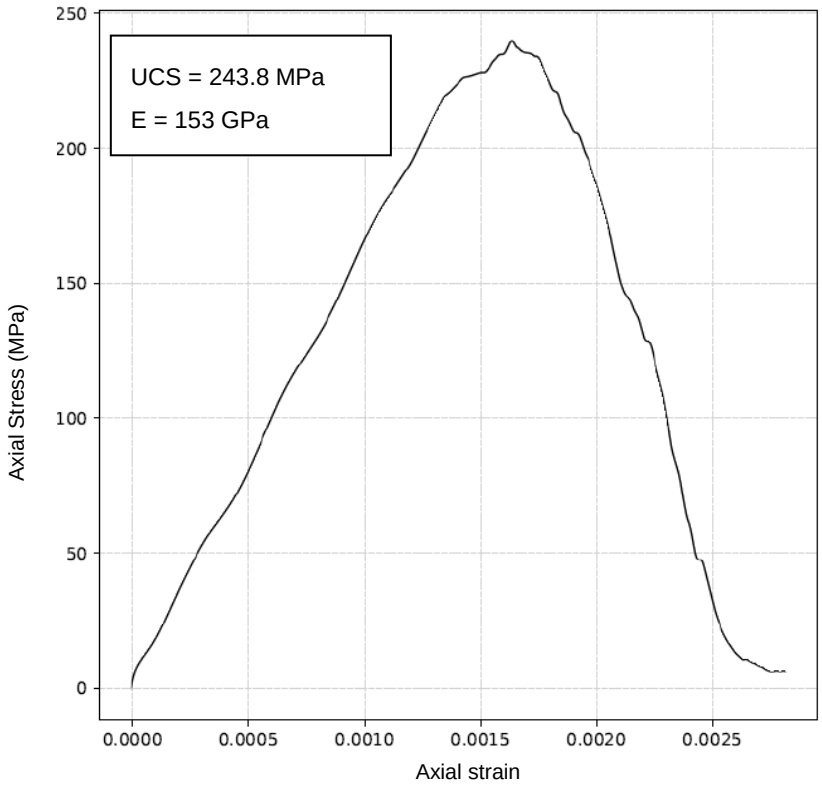

Figure 5. Stress-strain curve obtained with increasing particle size.

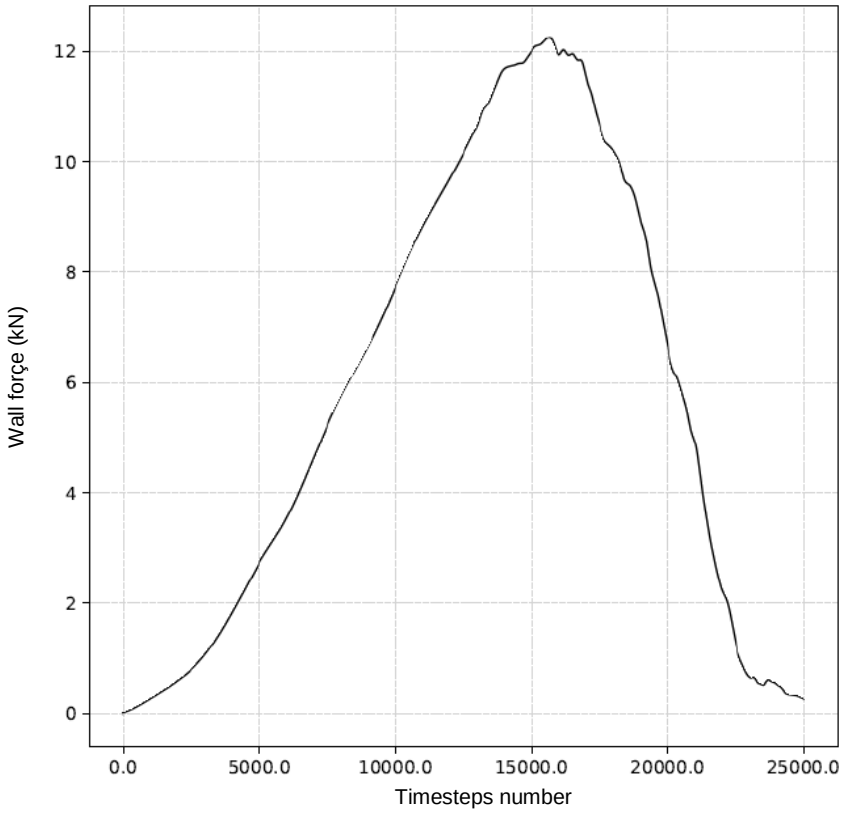

Figure 6. Time-series of net wall force with increasing particle size.

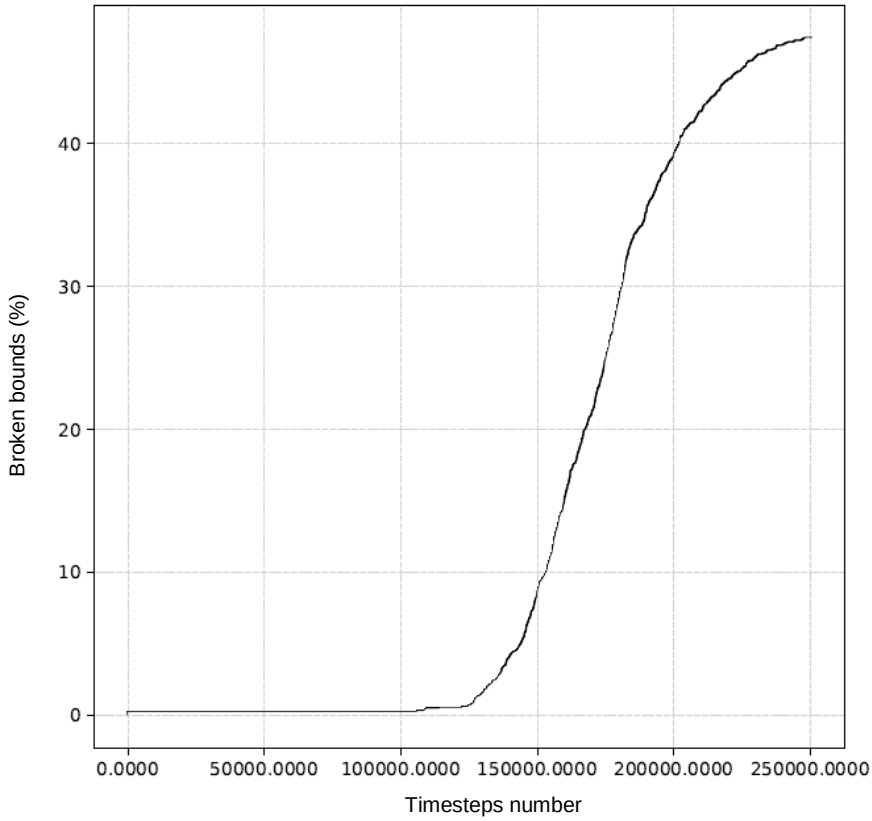

Figure 7. Time-series of percentage of bonds broken with increasing particle size.

We believe that the geomaterial sample no longer remains intact as before when we increase the particle size. Apparently, this is less expected in uniaxial compression laboratory experiments.

4.2 Speedup and Scalability of cores on CPU

For a fixed number of the particles in the prism rectangular, we record the computational time and compare the respective speedups using different number of processors n_p, which specifies the number of MPI parallel processes used in our simulation.

It was considered up to six physical CPU cores (Figure 8 and 9). The scalability of the parallel analysis was also investigated. The results are shown in Figure 9. For a certain processor number the speedup is defined as the simulation time using one single processor divided by that of specific number of processors.

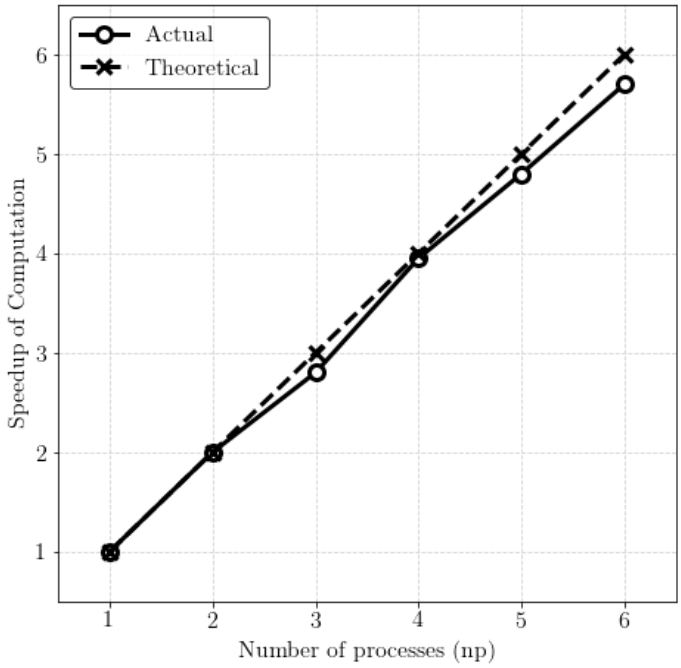

Figure 8. Speedup of calculus thought parallelization.

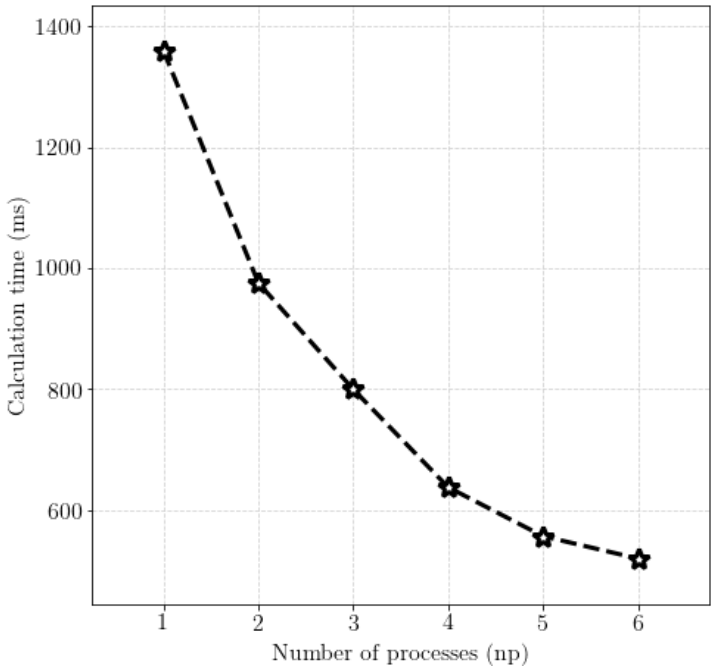

Figure 9. Scalability of cores on CPU.

According to Figures 8 and 9, the code presented efficient speedup and high scalability for parallel computing. Similar results were found in the literature. In addition, we believe that the number of physical cores could be the key to the performance of parallel computations.

5 CONCLUSIONS

This work describes the modeling of macroscopic properties in geomaterials samples using discrete elements and parallel computing. In a uniaxial compression experiments, a sample of geomaterial is slowly compressed by a piston until failure occurs. The numerical model sought to reproduce the experimental procedure. In the simulations realized were encountered the *Young's* modulus and the Unconfined Compressive Strength (UCS). Analytical relationship between the microphysical parameters and the macroscopic properties can be obtained by conducting a simulation campaign to fine tune these parameters so as to obtain suitable macroscopic properties. Additionally, the corresponding number of broken bonds and the wall force time-series are determined. We observed that the geomaterial sample remains largely intact even after the post-peak stress for a pre-set particle radius. This is exactly what one would expect in laboratory uniaxial compression experiments. However, the geomaterial sample becomes more susceptible to damage by increasing the particle size. This is less expected in uniaxial compression laboratory experiments. Anyway, considering the magnitude of the values in the simulations, it is possible to relate the sample of geomaterial analyzed with a rock material or a high strength concrete. Our simulations were carried out using open multi core processing and message passing interface code. The code was tested on personal computer with six CPU multi-core processor. Numerical results showed almost linear speedup and scalability for our parallelization evaluation scenarios which agree with literature. Future investigations will examine different types of geomaterials samples such as concretes and soils besides utilize in CPU processing a greater amount multi-core processor.

ACKNOWLEDGEMENTS

Thanks to Cilamce 2017 organizing committee for the opportunity.

REFERENCES

Cundall, P. A., Strack, O. D. L., 1979. A discrete numerical model for granular assemblies. *Geotechnique*, vol. 29, pp. 47–65.

Donzé, F. V., Richefeu, V., Magnier, S. A. 2009. Avances in Discrete Elemet Method Applied to Soil, Rock and Concrete Mechanics. *Electronic Journal of Geotechnical Engineering*, vol. 8, pp.44-88.

Hoang Tran, V. D. 2013. *A coupled finite-discrete element framework for soil-structure interaction analysis*. Tese de Doutorado. McGill University, Montréal, Québec, Canada.

Hwu, W. W. , Keutzer, K. 2008. *The Concurrency Challenge*. IEEE Design and Test of Computers, July/August, 312–320.

Munjiza, A. A., Knight, E. E., Rougier, E., 2012. *Computational Mechanics of Discontinua*, Wiley Series in Computational Mechanics. Chichester, UK: Wiley.

O'Sullivan, C., 2011. *Particulate Discrete Element Modelling: a Geomechanics Perspective*. New York: Spon Press.

Sakai, M., Yamada, Y., Shigeto, Y., Shibata, K., Kawasaki, V. M., Koshizuka, S., 2010. Large-scale DEM modeling in a fluidized bed. *Int. J. Num. Meth. in Fluids*, v. 64, pp. 19–35.

von Neumann, J., 1945. *First Draft of a Report on the EDVAC*. Contrato N°. W-670-ORD-4926, U.S. Army Artillery Department the and University of Pennsylvania. (reproduced in H. H. Goldstine, Ed., The Computer: From Pascal to von Neumann, Princeton University Press, Princeton, NJ, 1972).

Weatherley, D. K., Boros, V. E., Hancock, W. R., Abe, S., 2010. Scaling benchmark of ESyS-Particle for elastic wave propagation simulations. *IEEE Sixth International Conference on e-Science*, Brisbane, Australia, 7–10 December, pp. 277–283.

Weatherley, D. K., Boros, V. E., Hancock, W. R., Abe, S., 2014. *ESyS-particle Tutorial and User Guide Version 2.3.1*. The University of Queensland S. Abe, Institute for Geothermal Resource Management.